



Novel coumarin-6-sulfonamides as apoptotic anti-proliferative agents: synthesis, *in vitro* biological evaluation, and QSAR studies

Ahmed Sabt, Omaila M. Abdelhafez, Radwan S. El-Haggag, Hassan M. F. Madkour, Wagdy M. Eldehna, Ezz El-Din A. M. El-Khrisy, Mohamed A. Abdel-Rahman & Laila. A. Rashed

To cite this article: Ahmed Sabt, Omaila M. Abdelhafez, Radwan S. El-Haggag, Hassan M. F. Madkour, Wagdy M. Eldehna, Ezz El-Din A. M. El-Khrisy, Mohamed A. Abdel-Rahman & Laila. A. Rashed (2018) Novel coumarin-6-sulfonamides as apoptotic anti-proliferative agents: synthesis, *in vitro* biological evaluation, and QSAR studies, Journal of Enzyme Inhibition and Medicinal Chemistry, 33:1, 1095-1107, DOI: [10.1080/14756366.2018.1477137](https://doi.org/10.1080/14756366.2018.1477137)

To link to this article: <https://doi.org/10.1080/14756366.2018.1477137>



© 2018 The Author(s). Published by Informa UK Limited, trading as Taylor & Francis Group.



[View supplementary material](#)



Published online: 26 Jun 2018.



[Submit your article to this journal](#)



[View related articles](#)



[View Crossmark data](#)

RESEARCH PAPER



Novel coumarin-6-sulfonamides as apoptotic anti-proliferative agents: synthesis, *in vitro* biological evaluation, and QSAR studies

Ahmed Sabt^a, Omaima M. Abdelhafez^a, Radwan S. El-Haggar^b, Hassan M. F. Madkour^c, Wagdy M. Eldehna^d, Ezz El-Din A. M. El-Khrisy^a, Mohamed A. Abdel-Rahman^e and Laila. A. Rashed^f

^aChemistry of Natural Compounds Department, National Research Centre, Dokki, Egypt; ^bPharmaceutical Chemistry Department, Faculty of Pharmacy, Helwan University, Cairo, Egypt; ^cChemistry Department, Faculty of Science, Ain-shams University, Cairo, Egypt; ^dDepartment of Pharmaceutical Chemistry, Faculty of Pharmacy, Kafrelsheikh University, Kafrelsheikh, Egypt; ^eDepartment of Pharmaceutical Chemistry, Faculty of Pharmacy, Egyptian Russian University, Badr City, Cairo, Egypt; ^fDepartment of Biochemistry, Faculty of Medicine, Cairo University, Cairo, Egypt

ABSTRACT

Herein, we report the synthesis of different novel sets of coumarin-6-sulfonamide derivatives bearing different functionalities (**4a**, **b**, **8a–d**, **11a–d**, **13a**, **b**, and **15a–c**), and *in vitro* evaluation of their growth inhibitory activity towards the proliferation of three cancer cell lines; HepG2 (hepatocellular carcinoma), MCF-7 (breast cancer), and Caco-2 (colon cancer). HepG2 cells were the most sensitive cells to the influence of the target coumarins. Compounds **13a** and **15a** emerged as the most active members against HepG2 cells ($IC_{50} = 3.48 \pm 0.28$ and $5.03 \pm 0.39 \mu M$, respectively). Compounds **13a** and **15a** were able to induce apoptosis in HepG2 cells, as assured by the upregulation of the Bax and downregulation of the Bcl-2, besides boosting caspase-3 levels. Besides, compound **13a** induced a significant increase in the percentage of cells at Pre-G1 by 6.4-folds, with concurrent significant arrest in the G2-M phase by 5.4-folds compared to control. Also, **13a** displayed significant increase in the percentage of annexin V-FITC positive apoptotic cells from 1.75–13.76%. Moreover, QSAR models were established to explore the structural requirements controlling the anti-proliferative activities.

ARTICLE HISTORY

Received 22 March 2018
Revised 10 May 2018
Accepted 10 May 2018

KEYWORDS

Anticancer; Apoptosis;
Coumarin-6-sulfonamides;
2D-QSAR; Synthesis

Introduction

Cancer is a very complex, widespread and lethal disease that affects approximately 14 million people every year. In 2018, the American Cancer Society predict that the new diagnosed cancer cases will reach to 1,735,350 and cancer death 595,690 cancer deaths in the United States¹. Accordingly, the discovery of new anti-cancer agents with promising bioactivity and high therapeutic index is still an urgent need and a major challenge for researchers.



It is well established that natural and synthetic coumarin derivatives have attracted a great deal of interest due to their variety of biological and pharmacological properties, such as their anti-inflammatory², antibacterial³, antiviral⁴, and anti-cancer activities⁵. In the current medical era, much attention has been extensively paid to modify and update coumarin-based drug leads from the point of view of drug design and medicinal chemistry to fulfill more effective and safe anti-cancer agents^{6–8}.


The promising biological profile of coumarins as anti-cancer agents, and their easy synthetic modifications paved the way for design and synthesis of various coumarin-based derivatives with diverse activities against cancer. In this context, many coumarin-based molecules were widely reported to possess anti-cancer activity through binding to different targets and diverse pharmacological mechanisms, to name just a few, selective estrogen receptor modulation^{9–11} (as CHF4227, Figure 1), MEK1

inhibition^{12–14} (as G8935, Figure 1), steroid sulfatase inhibition^{15–17} (as Irosustat, Figure 1), CDC25 phosphatases inhibition^{18–20} (as SV37, Figure 1), tubulin polymerization inhibition^{21–23}, aromatase inhibition^{24,25}, COX-2 inhibition²⁶, and apoptosis induction^{27–31}.

On the other hand, sulfonamide derivatives constitute another important class of organic compounds that displayed interesting biological activities including anti-carbonic anhydrase and anti-cancer activities^{32,33}. It is noteworthy to mention that there is a continuing interest in the synthesis of coumarin sulfonamide derivatives as potent anti-cancer agents^{34–37}. SLC-0111, Figure 1, an ureido benzenesulfonamide derivative, is currently in phase I/II clinical trials as anti-cancer drug. SLC-0111 II is characterized by its selectivity towards inhibition of the transmembrane isoforms hCA IX/XII (over the cytosolic isoforms hCA I/II). SLC-0111 was also able to block human breast cancer invasion, delay tumor growth and diminish the cancer stem cell population *in vivo*^{38–40}.

KCN1, Figure 1, a novel synthetic sulfonamide, is a HIF pathway inhibitor with *in vitro* and *in vivo* anti-pancreatic cancer activities and preclinical pharmacology. KCN1 specifically inhibited HIF reporter gene activity in several glioma cell lines at the nanomolar level. Also, KCN1 effectively inhibited the growth of subcutaneous malignant glioma tumor xenografts with low side effects on the host^{41,42}. Moreover, Indisulam (*N*-(3-chloro-7-indolyl)-1,4-benzene-disulfonamide), Figure 1, is an orally active sulfonamide anti-tumor

CONTACT Wagdy M. Eldehna  wagdy2000@gmail.com  Department of Pharmaceutical Chemistry, Faculty of Pharmacy, Kafrelsheikh University, Kafrelsheikh, Egypt

 Supplemental data for this article can be accessed [here](#).

© 2018 The Author(s). Published by Informa UK Limited, trading as Taylor & Francis Group.

This is an Open Access article distributed under the terms of the Creative Commons Attribution License (<http://creativecommons.org/licenses/by/4.0/>), which permits unrestricted use, distribution, and reproduction in any medium, provided the original work is properly cited.

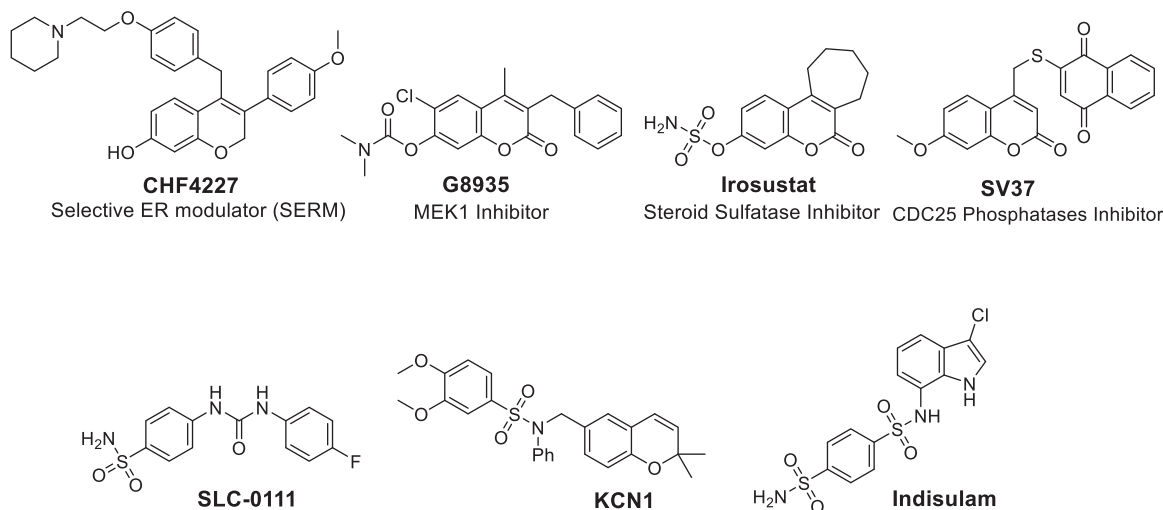


Figure 1. Structure of some reported coumarins and sulfonamides with effective anti-cancer activities.

agent that possesses anti-cancer properties through down-regulation of various cell-cycle checkpoint molecules, thereby blocking the phosphorylation of retinoblastoma protein and inducing p53 and p21. Pre-clinical and clinical studies have established synergy of Indisulam with nucleoside analogs as well as topoisomerase inhibitors^{43–47}.

Based on the aforementioned findings, herein we report the synthesis of novel sets of coumarin sulfonamide derivatives (**4a**, **b**, **8a–d**, **11a–d**, **13a**, **b** and **15a–c**) and their *in vitro* growth inhibitory activity towards the proliferation of three cancer cell lines; HepG2 (hepatocellular carcinoma), MCF-7 (breast cancer), and Caco-2 (colon cancer). Additionally, the synthesized coumarin sulfonamides were further examined regarding their potential apoptotic induction and their effects on cell cycle progression in the Hep-G2 cancer cells to acquire a perception for the mechanism of their anti-cancer activity.

Materials and methods

Chemistry

Melting points were determined on Electrothermal IA 9000 apparatus and were uncorrected. Elemental microanalyses were performed on Elementar, Vario EL, at the Micro-analytical Laboratory, National Research Centre, Dokki, Cairo. The ¹H NMR and ¹³C NMR spectra were recorded with a BrukerAvance 400 MHz spectrometer at Turku University, Finland and JEOL ACA 500 NMR spectrometer, at the National Research Centre, Dokki, Cairo, Egypt. The mass spectra were performed on Mass Spectrometer Finnigan MAT SSQ-7000 and GCMS-QP 1000EX Shimadzu Gas Chromatography MS Spectrometer at Faculty of Science, Cairo University, Egypt. The reactions were followed by TLC (silica gel, aluminum sheets 60 F254, Merck) using chloroform/methanol (9.5:0.5 v/v) as eluent.

Synthesis of coumarin-6-sulfonyl chloride **2**

Compound 2-oxo-2H-chromene-6-sulfonyl chloride **2** was obtained from a reaction of coumarin with chlorosulfonic acid⁴⁸.

Synthesis of coumarin-6-sulfonamide derivatives **4a,b**

A solution of 2-oxo-2H-chromene-6-sulfonyl chloride **2** (0.5 g, 2 mmol) and the appropriate sulfanilamide **3a** or sulfapyridine **3b**

(2 mmol) in absolute ethanol (25 ml) was refluxed for 12 h. The obtained solid was filtered, dried, and recrystallized from ethanol to give compounds **4a**, **b**.

2-Oxo-N-(4-sulfamoylphenyl)-2H-chromene-6-sulfonamide (**4a**)

Brown crystals, mp 266–268 °C, yield (43%). ¹H NMR (500 MHz, DMSO-d₆) δ ppm: 6.47 (d, 1H, *J* = 9.5 Hz, H3 of coumarin), 6.94 (d, 2H, *J* = 8.2 Hz, Ar), 7.31 (d, 1H, *J* = 8.5 Hz, H8 of coumarin), 7.61 (d, 2H, *J* = 8.4 Hz, Ar), 7.71–7.71 (m, 3H, NH₂ and H7 of coumarin), 7.95 (d, 1H, *J* = 10 Hz, H4 of coumarin), 8.11 (s, 1H, H5 of coumarin), 10.95 (s, 1H, NH); ¹³C NMR (100 MHz, DMSO-d₆); δ ppm: 116.32 (2C), 116.90, 118.40, 118.84, 125.96, 125.97, 127.87 (2C), 129.81 (2C), 137.55, 144.94 (C4 of coumarin), 153.88 (C9 of coumarin), 160.40 (C=O of coumarin); MS *m/z* [%]: 380 [9.21], 92 [100]. Analysis for C₁₅H₁₂N₂O₆S₂ (380), Calcd.: % C, 47.36; H, 3.18; N, 7.36; O, 25.24; S, 16.86. Found: % C, 47.28; H, 3.22; N, 7.42; O, 25.18; S, 16.78.

2-Oxo-N-(4-(N-(pyridin-2-yl)sulfamoyl)phenyl)-2H-chromene-6-sulfonamide (**4b**)

White crystals, mp 237–239 °C, yield (40%). ¹H NMR (400 MHz, DMSO-d₆) δ ppm: 6.62 (d, 1H, *J* = 9.6 Hz, H3 of coumarin), 6.83 (t, 1H, *J* = 12.4 Hz, H3 of pyridine), 7.08 (d, 1H, *J* = 8.8 Hz, H5 of pyridine), 7.24 (d, 2H, *J* = 8.8 Hz, Ar), 7.55 (d, 1H, *J* = 8.8 Hz, H8 of coumarin), 7.67 (t, 1H, *J* = 8.8 Hz, H4 of pyridine), 7.75 (d, 2H, *J* = 8.8 Hz, Ar), 7.94–7.96 (m, 2H, H2 of pyridine and H7 of coumarin), 8.15 (d, 1H, *J* = 10 Hz, H4 of coumarin), 8.28 (s, 1H, H5 of coumarin), 11.05 (s, 1H, NH, D₂O exchangeable), 11.92 (s, 1H, NH, D₂O exchangeable); ¹³C NMR (100 MHz, DMSO); δ ppm: 114.23 (C5 of pyridine), 118.42 (2C), 118.99 (2C), 119.49, 128.29, 128.66, 128.55, 129.88, 129.96, 135.38, 137.18, 140.90, 141.01, 141.29, (Ar, pyridine and coumarin), 143.76 (C4 of coumarin), 153.57 (C=N of pyridine), 156.51 (C9 of coumarin), 159.54 (C=O of coumarin); Analysis for C₂₀H₁₅N₃O₆S₂ (457), Calcd.: % C, 52.51; H, 3.30; N, 9.19; O, 20.98; S, 14.02. Found: % C, 52.58; H, 3.40; N, 9.22; O, 21.01; S, 14.09.

Synthesis of N-(4-acetylphenyl)-2-oxo-2H-chromene-6-sulfonamide (**6**)

Compound **6** was prepared according to the literatures procedures⁴⁹.

Synthesis of schiff base coumarin sulfonamides 8a-d

To a mixture of compound **6** (0.25 g, 0.729 mmol) and the appropriate phenylhydrazine **7a**, 2,4-dinitrophenylhydrazine **7b**, 2,4,6-trichlorophenylhydrazine **7c** or *p*-toluenesulfonyl hydrazide **7d** (0.911 mmol) in absolute ethanol (30 ml), three drops of glacial acetic acid was added and the reaction mixture was refluxed for 8 h. After cooling, the precipitate was filtered, washed with water, purified *via* crystallization from ethanol to give compounds **8a-d**, respectively.

2-Oxo-N-(4-(1-(2-phenylhydrazono)ethyl)phenyl)-2H-chromene-6-sulfonamide (8a)

Brown crystals, mp 178–180 °C, yield (66%). ¹H NMR (500 MHz, DMSO-d₆) δ ppm: 2.19 (s, 3H, CH₃), 6.47 (d, 1H, *J* = 12 Hz, H3 of coumarin), 6.87–7.83 (m, 11H, NH, Ar, and H8 of coumarin), 7.95 (dd, 1H, *J* = 6 and 10.5 Hz, H7 of coumarin), 8.04 (d, 1H, *J* = 2.4 Hz, H4 of coumarin), 8.23 (s, 1H, H5 of coumarin), 11.09 (s, 1H, NH); ¹³C NMR (125 MHz, DMSO); δ ppm: 13.10 (CH₃), 113.21 (2C), 113.25, 118.59, 119.25, 120.47, 122.66, 126.50, 128.18, 128.29, 129.32 (2C), 129.40, 130.33 (2C), 132.62, 135.93, 135.95, 143.81 (C4 of coumarin), 154.54 (C=N), 156.31 (C9 of coumarin), 160.02 (C=O of coumarin); HRMS (ESI): *m/z* calculated for C₂₃H₁₉N₃O₄S [M + H]⁺, 434.1169; found, 434.1163.

N-(4-(1-(2-(2,4-dinitrophenyl)hydrazono)ethyl)phenyl)-2-oxo-2H-chromene-6-sulfonamide (8b)

Red crystals, mp 269–270 °C, yield (60%). ¹H NMR (500 MHz, DMSO-d₆) δ ppm: 2.36 (s, 3H, CH₃), 5.72 (s, 1H, NH), 6.61 (d, 1H, *J* = 6.50 Hz, H3 of coumarin), 7.21 (d, 2H, *J* = 11 Hz, Ar), 7.57–7.85 (m, 3H, Ar, and H8 of coumarin), 7.96 (dd, 1H, *J* = 2.5 and 2.5 Hz, H7 of coumarin), 8.03 (d, 1H, *J* = 12 Hz, H4 of coumarin), 8.19 (d, 1H, *J* = 12 Hz, Ar), 8.29 (s, 1H, H5 of coumarin), 8.36 (d, 1H, *J* = 12 Hz, NO₂-CH, Ar), 8.87 (s, 1H, H3 of 2,4-(NO₂)₂C₆H₃), 11.06 (s, 1H, NH); ¹³C NMR (125 MHz, DMSO-d₆); δ ppm: 13.83 (CH₃), 118.26, 118.29, 118.38, 118.42, 118.60, 119.41, 119.50, 120.01, 127.26, 128.18, 128.29, 130.00, 130.05, 130.31, 132.60, 135.88, 138.33, 142.38, 143.86 (C4 of coumarin), 154.37 (C=N), 156.34 (C9 of coumarin), 159.56 (C=O of coumarin); Analysis for C₂₃H₁₇N₅O₈S (523), Calcd.: % C, 52.77; H, 3.27; N, 13.38; O, 24.45; S, 6.13. Found: % C, 52.84; H, 3.20; N, 13.32; O, 24.40; S, 6.18.

2-Oxo-N-(4-(1-(2-(2,4,6-trichlorophenyl)hydrazono)ethyl)phenyl)-2H-chromene-6-sulfonamide (8c)

White crystals, mp 259–260 °C, yield (58%). ¹H NMR (500 MHz, DMSO-d₆) δ ppm: 2.21 (s, 3H, CH₃), 6.55 (d, 1H, *J* = 12 Hz, H3 of coumarin), 7.11 (d, 2H, *J* = 10.5 Hz, Ar), 7.54–7.60 (m, 3H, Ar, and H8 of coumarin), 7.64 (s, 2H, H3 and H5 of 2,4,6-(Cl)₃C₆H₂), 7.92 (dd, 1H, *J* = 2 and 2 Hz, H7 of coumarin), 8.04 (s, 1H, NH), 8.16 (d, 1H, *J* = 12.5 Hz, H4 of coumarin), 8.22 (s, 1H, H5 of coumarin), 10.51 (s, 1H, NH); ¹³C NMR (125 MHz, DMSO-d₆); δ ppm: 12.98 (CH₃), 118.23, 118.29, 118.36, 119.39, 120.21 (2C), 126.78 (2C), 128.06, 128.17, 128.86, 129.14 (2C), 130.03, 134.92, 135.86, 137.80, 139.14, 143.85 (C4 of coumarin), 145.64 (C=N), 156.33 (C9 of coumarin), 159.54 (C=O of coumarin); Analysis for C₂₃H₁₆Cl₃N₃O₄S (534), Calcd.: % C, 51.46; H, 3.00; Cl, 19.81; N, 7.83; O, 11.92; S, 5.97. Found: % C, 51.49; H, 2.96; Cl, 19.85; N, 7.85; O, 11.87; S, 5.92.

2-Oxo-N-(4-(1-(2-tosylhydrazono)ethyl)phenyl)-2H-chromene-6-sulfonamide (8d)

White crystals, mp 163–165 °C, yield (76%). ¹H NMR (400 MHz, DMSO-d₆) δ ppm: 2.03 (s, 3H, CH₃), 2.31 (s, 3H, CH₃ - tosyl), 6.60 (d, 1H, *J* = 9.6 Hz, H3 of coumarin), 7.11 (d, 2H, *J* = 8.4 Hz, Ar), 7.39 (d, 2H, *J* = 8.4 Hz, Ar-tosyl), 7.50–7.56 (m, 3H, Ar, and H8 of coumarin), 7.78 (d, 2H, *J* = 8.4 Hz, Ar-tosyl), 7.91 (dd, 1H, *J* = 2 and 2 Hz, H7 of coumarin), 8.17 (d, 1H, *J* = 9.6 Hz, H4 of coumarin), 8.18 (s, 1H, H5 of coumarin), 10.44 (s, 1H, NH), 10.56 (s, 1H, NH); ¹³C NMR (100 MHz, DMSO); δ ppm: 14.47 (CH₃), 21.47 (CH₃), 118.30, 118.45, 118.53, 119.42, 119.75, 125.77, 127.50, 128.04 (2C), 128.18, 129.91, 129.97 (2C), 133.45, 135.70, 136.57, 138.90, 143.79, 143.83 (C4 of coumarin), 152.92 (C=N), 156.37 (C9 of coumarin), 159.56 (C=O of coumarin); Analysis for C₂₄H₂₁N₃O₆S₂ (511), Calcd.: % C, 56.35; H, 4.14; N, 8.21; O, 18.77; S, 12.54. Found: % C, 56.40; H, 4.08; N, 8.16; O, 18.71; S, 12.50.

2-(1-(4-(2-Oxo-2H-chromene-6-sulfonamido)phenyl)ethylidene)hydrazine carbothioamide (9)

A mixture of *N*-(4-acetylphenyl)-2-oxo-2H-chromene-6-sulfonamide **6** (0.5 g, 1.45 mmol), and thiosemicarbazide (1.45 mmol) in absolute ethanol (20 ml) and catalytic amount of acetic acid was refluxed for 6 h. The obtained solid was filtered, dried, and washed with hot ethanol to afford compound **9**.

Light yellow crystals, mp 253–254 °C, yield (34%). ¹H NMR (400 MHz, DMSO-d₆) δ ppm: 2.18 (s, 3H, CH₃), 6.58 (d, 1H, *J* = 4.4 Hz, H3 of coumarin), 7.25 (d, 2H, *J* = 6.8 Hz, Ar), 7.55 (d, 1H, *J* = 2.4 Hz, H8 of coumarin), 7.79–7.84 (m, 4H, NH₂, Ar), 7.94 (dd, 1H, *J* = 6 and 1.6 Hz, H7 of coumarin), 8.16 (d, 1H, *J* = 10 Hz, H4 of coumarin), 8.29 (d, 1H, *J* = 2.4 Hz, H5 of coumarin), 10.13 (s, 1H, NH), 10.60 (s, 1H, NH); ¹³C NMR (100 MHz, DMSO-d₆); δ ppm: 14.17 (CH₃), 113.57, 118.30, 118.34, 119.43 (2C), 119.69, 128.14 (2C), 130.01, 133.82, 135.86, 138.72, 143.82 (C4 of coumarin), 147.53 (C=N), 156.36 (C9 of coumarin), 159.54 (C=O of coumarin), 179.22 (C=S); Analysis for C₁₈H₁₆N₄O₄S₂ (416), Calcd.: % C, 51.91; H, 3.87; N, 13.45; O, 15.37; S, 15.40. Found: %C, 51.79; H, 3.82; N, 13.31; O, 15.42; S, 15.47.

General procedures for preparation of target compounds (11a–d and 13a, b)

A mixture of thiosemicarbazone **9** (10 mmol) and the appropriate α -halocarbonyl compounds **10a–d**, phenacyl bromide **12a** or coumarin-3-acetyl bromide **12b** (10 mmol) in dioxane (25 ml) containing catalytic amount of triethylamine was heated under reflux for 8 h and then cooled. The solution was poured onto water-ice and concentrated hydrochloric acid. The solid produced was collected by filtration and crystallized from ethanol to furnish compounds **11a–d** and **13a, b**, respectively.

N-(4-(1-(2-(4-methylthiazol-2-yl)hydrazono)ethyl)phenyl)-2-oxo-2H-chromene-6-sulfonamide (11a)

Brown crystals, mp 257–259 °C, yield (78%). ¹H NMR (500 MHz, DMSO-d₆) δ ppm: 2.15 (s, 3H, CH₃), 2.45 (s, 3H, CH₃-thiazole), 5.99 (s, 1H, CH thiazole), 6.57 (d, 1H, *J* = 9.6 Hz, H3 of coumarin), 7.19 (d, 2H, *J* = 8.6 Hz, Ar), 7.52 (d, 1H, *J* = 8.6 Hz, H8 of coumarin), 7.80 (d, 2H, *J* = 8.6 Hz, Ar), 7.91 (dd, 1H, *J* = 9.5 and 2 Hz, H7 of coumarin), 8.12 (d, 1H, *J* = 10 Hz, H4 of coumarin), 8.27 (s, 1H, H5 of coumarin), 10.55 (s, 1H, NH, D₂O exchangeable), 11.01 (s, 1H, NH, D₂O exchangeable); ¹³C NMR (125 MHz, DMSO); δ ppm: 13.83 (CH₃), 14.55 (CH₃-thiazole), 118.26, 118.42, 118.60, 119.41, 119.50, 120.01, 127.26, 128.18, 130.31, 132.60, 135.88, 138.33, 142.38

(Ar, C5-thiazole and coumarin), 143.86 (C4 of coumarin), 154.33 (C=N), 154.37 (C4-thiazole), 156.34 (C9 of coumarin), 159.56 (C=O of coumarin), 168.66 (S-C=N): Analysis for $C_{21}H_{18}N_4O_4S_2$ (454), Calcd.: % C, 55.49; H, 3.99; N, 12.33; O, 14.08; S, 14.11. Found: % C, 55.40; H, 3.96; N, 12.36; O, 14.05; S, 14.14.

Ethyl 4-methyl-2-(2-(1-(4-(2-oxo-2H-chromene-6-sulfonamido)phenyl) ethylidene)hydrazinyl)thiazole-5-carboxylate (11b)

Yellow crystals, mp 180–182 °C, yield (53%). 1H NMR (500 MHz, DMSO- d_6) δ ppm: 1.21 (t, 3H, J = 11.48 Hz, CH_3), 2.19 (s, 3H, CH_3), 2.41 (s, 3H, CH_3 -thiazole), 4.14 (q, 2H, J = 6.65 Hz, OCH_2), 6.56 (d, 1H, J = 9.2 Hz, H3 of coumarin), 7.14 (d, 2H, J = 8.4 Hz, Ar), 7.53 (d, 1H, J = 8.6 Hz, H8 of coumarin), 7.63 (d, 2H, J = 8.4 Hz, Ar), 7.91 (dd, 1H, J = 9.6 and 5 Hz, H7 of coumarin), 8.14 (d, 1H, J = 9.6 Hz, H4 of coumarin), 8.22 (s, 1H, H5 of coumarin), 10.67 (s, 1H, NH), 11.04 (s, 1H, NH); ^{13}C NMR (125 MHz, DMSO- d_6); δ ppm: 14.62 (CH_3), 14.87 (CH_3), 26.93 (CH_3 -ester), 60.69 (OCH_2), 112.87, 118.34, 118.67, 119.48, 120.01, 127.51, 128.25, 130.13 (2C), 130.37, 135.91 (Ar, C5-thiazole and coumarin), 143.87 (C4 of coumarin), 152.41 (C=N), 156.41 (C4-thiazole), 156.53 (C9 of coumarin), 159.48 (C=O of coumarin), 169.66 (S-C=N), 185.45 (C=O); HRMS (ESI): m/z calculated for $C_{24}H_{22}N_4O_4S_2$ [$M + H$] $^+$, 527.1054; found, 527.1052.

N-(4-(1-(2-(5-((4-chlorophenyl)diazanyl)-4-methylthiazol-2-yl)hydrazono)ethyl) phenyl)-2-oxo-2H-chromene-6-sulfonamide (11c)

Red crystals, mp 250–252 °C, yield (88%). 1H NMR (500 MHz, DMSO- d_6) δ ppm: 2.41 (s, 3H, CH_3), 2.57 (s, 3H, CH_3 -thiazole), 6.62 (d, 1H, J = 12 Hz, H3 of coumarin), 7.21 (d, 2H, J = 10.5 Hz, Ar), 7.35–7.39 (m, 4H, Ar), 7.59 (d, 1H, J = 8.6 Hz, H8 of coumarin), 7.85 (d, 2H, J = 8.8 Hz, Ar), 7.97 (dd, 1H, J = 3 and 3 Hz, H7 of coumarin), 8.19 (d, 1H, J = 12 Hz, H4 of coumarin); 8.30 (s, 1H, H5 of coumarin), 10.65 (br, 2H, 2NH); ^{13}C NMR (125 MHz, DMSO) δ ppm: 14.55 (CH_3), 15.50 (CH_3), 118.35, 118.38, 118.64, 119.47 (2C), 119.98, 123.52, 124.53, 128.22, 128.54, 129.64 (2C), 129.99, 130.04, 130.31, 133.07, 135.92, 139.30, 140.32 (Ar, C5-thiazole and coumarin), 143.84 (C4 of coumarin), 147.89 (C4-thiazole), 151.37 (C=N), 156.42 (C9 of coumarin), 159.54 (C=O of coumarin), 171.80 (S-C=N); Analysis for $C_{27}H_{21}ClN_6O_4S_2$ (592), Calcd.: % C, 54.68; H, 3.57; Cl, 5.98; N, 14.17; O, 10.79; S, 10.81. Found: % C, 54.61; H, 3.52; N, 14.20; O, 10.71; S, 10.70.

N-(4-(1-(2-(4-methyl-5-(p-tolyldiazanyl)thiazol-2-yl)hydrazono)ethyl)phenyl)-2-oxo-2H-chromene-6-sulfonamide (11d)

Red crystals, mp 258–259 °C, yield (83%). 1H NMR (500 MHz, DMSO- d_6) δ ppm: 2.25 (s, 3H, CH_3), 2.41 (s, 3H, CH_3), 2.56 (s, 3H, CH_3 -thiazole), 6.62 (d, 1H, J = 12 Hz, H3 of coumarin), 7.13 (d, 2H, J = 10 Hz, Ar), 7.20–7.25 (m, 4H, Ar), 7.59 (d, 1H, J = 11 Hz, H8 of coumarin), 7.85 (d, 2H, J = 10.5 Hz, Ar), 7.97 (dd, 1H, J = 3 and 3 Hz, H7 of coumarin), 8.19 (d, 1H, J = 12 Hz, H4 of coumarin), 8.29 (s, 1H, H5 of coumarin), 10.47 (s, 1H, NH), 10.77 (s, 1H, NH); ^{13}C NMR (125 MHz, DMSO); δ ppm: 15.48 (CH_3), 16.94 (CH_3), 20.85 (CH_3), 114.68, 118.39, 118.60, 119.47 (2C), 128.23, 128.28, 128.52, 129.99, 130.04, 130.20, 130.33, 131.65, 133.26, 135.63, 135.83, 137.96, 140.10, 141.61, 142.35 (Ar, thiazole and coumarin), 143.83 (C4 of coumarin), 151.15 (C=N), 156.44 (C9 of coumarin), 159.54 (C=O of coumarin), 171.79 (S-C=N); Analysis for $C_{28}H_{24}N_6O_4S_2$ (572),

Calcd.: % C, 58.73; H, 4.22; N, 14.68; O, 11.18; S, 11.20. Found: % C, 58.82; H, 4.14; N, 14.77; O, 11.19; S, 11.16.

2-Oxo-N-(4-(1-(2-(4-phenylthiazol-2-yl)hydrazono)ethyl)phenyl)-2H-chromene-6-sulfonamide (13a)

Yellow crystals, mp 170–171 °C, yield (80%). 1H NMR (500 MHz, DMSO- d_6) δ ppm: 2.19 (3H, s, CH_3), 6.56 (d, 1H, J = 5.75 Hz, H3 of coumarin), 7.16 (d, 2H, J = 8.8 Hz, Ar), 7.27–7.36 (m, 5H, Ar), 7.54 (d, 1H, J = 8.65 Hz, H8 of coumarin), 7.61 (d, 2H, J = 8.4 Hz, Ar), 7.94 (dd, 1H, J = 2.4 and 8 Hz, H7 of coumarin), 8.15 (d, 1H, J = 8 Hz, H4 of coumarin), 8.20 (s, 1H-thiazole), 8.29 (d, 1H, J = 2.5 Hz, H5 of coumarin), 10.59 (s, 1H, NH), 10.99 (s, 1H, NH); ^{13}C NMR (125 MHz, DMSO- d_6); δ ppm: 14.29 (CH_3), 104.44 (C4-thiazole), 118.29, 118.58, 119.43, 120.11, 125.96, 128.20, 128.29, 129.06 (2C), 130.05, 130.33, 132.61, 134.20, 135.21, 135.61, 135.86, 138.26, 142.35 (Ar, and coumarin), 143.86 (C4 of coumarin), 146.27 (C5-thiazole), 156.36 (C=N), 156.50 (C9 of coumarin), 159.56 (C=O of coumarin), 170.21 (S-C=N); MS m/z [%]: 516 [93], 132 [100]; Analysis for $C_{26}H_{20}N_4O_4S_2$ (516), Calcd.: % C, 60.45; H, 3.90; N, 10.85; O, 12.39; S, 12.41 Found: % C, 60.39; H, 3.88; N, 10.87; O, 12.33; S, 12.36.

2-Oxo-N-(4-(1-(2-(4-(2-oxo-2H-chromen-3-yl)thiazol-2-yl)hydrazono)ethyl)phenyl)-2H-chromene-6-sulfonamide (13b)

Yellow crystals, mp 201–202 °C, yield (63%). 1H NMR (500 MHz, DMSO- d_6) δ ppm: 2.16 (s, 3H, CH_3), 6.58 (d, 1H, J = 9.3 Hz, H3 of coumarin), 7.20 (d, 2H, J = 8.1 Hz, Ar), 7.34–8.80 (m, 7H, 8H coumarin and Ar), 7.97 (dd, 1H, J = 8.6 and 9.5 Hz, H7 of coumarin), 8.11 (s, 1H, H4 of coumarin), 8.15 (d, 1H, J = 9.5 Hz, H4 of coumarin), 8.28 (d, 1H, J = 8.6 Hz, H5 of coumarin), 8.52 (s, 1H-thiazole), 10.60 (s, 1H, NH); 10.99 (s, 1H, NH); ^{13}C NMR (125 MHz, DMSO- d_6); δ ppm: 14.32 (CH_3), 111.46 (C4-thiazole), 116.36, 118.30, 118.43, 118.58 (2C), 119.50, 120.05, 125.20, 127.17, 128.29, 129.20 (2C), 129.98, 130.33 (2C), 132.61, 134.03, 135.61, 135.84, 142.35, 143.80 (C4 of coumarin), 152.75 (C=N), 156.36 (C5-thiazole), 156.50 (2C9 of coumarin), 159.51 (2C=O of coumarin), 169.67 (S-C=N); Analysis for $C_{29}H_{20}N_4O_6S_2$ (584), Calcd.: % C, 59.58; H, 3.45; N, 9.58; O, 16.42; S, 10.97. Found: % C, 59.52; H, 3.48; N, 9.56; O, 16.36; S, 10.94.

General procedures for synthesis of thiazolidinones (15a–c)

In 50 ml round-bottom flask, thiosemicarbazone **9** (10 mmol) was dissolved in 15 ml acetic acid, followed by addition of anhydrous sodium acetate (30 mmol) under magnetic stirring and warming. After 20 min, bromoacetic acid **14a**, 2-bromopropanoic acid **14b** or maleic anhydride **14c** (15 mmol) was added and the reaction mixture was maintained under reflux for 8 h. After cooling, the precipitate was filtered, washed with water, dried, and recrystallized from ethanol to give compounds **15a–c**, respectively.

2-Oxo-N-(4-(1-(2-(5-oxo-4,5-dihydrothiazol-2-yl)hydrazono)ethyl)phenyl)-2H-chromene-6-sulfonamide (15a)

Yellow crystals, mp 191–192 °C, yield (64%). 1H NMR (400 MHz, $CDCl_3$) δ ppm: 2.23 (s, 3H, CH_3), 3.8 (s, 2H, CH_2 , thiazolidinone), 6.62 (d, 1H, J = 10.8 Hz, H3 of coumarin), 7.25 (d, 2H, J = 12 Hz, Ar), 7.55 (d, 1H, J = 8.4 Hz, H8 of coumarin); 7.85 (d, 2H, J = 8.4 Hz, Ar), 7.95 (dd, 1H, J = 2.4 and 2 Hz, H7 of coumarin), 8.16 (d, 1H, J = 10 Hz, H4 of coumarin), 8.29 (s, 1H, H5 of coumarin), 10.66 (s, 1H, NH), 10.97 (s, 1H, NH); ^{13}C NMR (100 MHz, $CDCl_3$);

δ ppm: 15.33 (CH₃), 56.30 (CH₂), 118.39, 118.64 (2C), 119.72, 127.93, 128.26, 129.99 (2C), 130.30, 132.66, 135.87, 142.35, 143.79 (C4 of coumarin), 152.56 (C=N), 156.50 (C9 of coumarin), 159.48 (C=O of coumarin), 166.33 (S-C=N), 196.90 (C=O); Analysis for C₂₀H₁₆N₄O₅S₂ (456), Calcd.: % C, 52.62; H, 3.53; N, 12.27; O, 17.52; S, 14.05. Found: % C, 52.58; H, 3.50; N, 12.19; O, 17.50; S, 14.00.

***N*-(4-(1-(2-(4-methyl-5-oxo-4,5-dihydrothiazol-2-yl)hydrazono)ethyl)phenyl)-2-oxo-2H-chromene-6-sulfonamide (15b)**

Brown crystals, mp 180–182 °C, yield (50%). ¹H NMR (400 MHz, CDCl₃) δ ppm: 1.59 (d, 3H, *J* = 9 Hz, CH₃ thiazolidinone), 2.27 (s, 3H, CH₃), 3.96 (q, 1H, *J* = 9 Hz CH thiazolidinone), 5.23 (s, 1H, NH), 6.44 (d, 1H, *J* = 10 Hz, H3 of coumarin), 7.05 (d, 2H, *J* = 10.5 Hz, Ar), 7.30 (d, 1H, *J* = 10.5 Hz, H8 of coumarin), 7.61 (d, 1H, *J* = 12 Hz, H4 of coumarin), 7.69 (d, 2H, *J* = 10.5 Hz, Ar), 7.84 (dd, 1H, *J* = 5.5 and 3 Hz, H7 of coumarin), 7.95 (s, 1H, H5 of coumarin), 11.02 (s, 1H, NH); ¹³C NMR (100 MHz, CDCl₃); δ ppm: 13.70 (CH₃), 18.17 (CH₃), 41.47 (CH of thiazolidinone), 117.10, 117.49, 117.88, 119.85 (2C), 126.66, 127.03 (2C), 129.05, 134.25, 136.40, 140.69, 141.30 (C4 of coumarin), 148.51 (C=N), 155.60 (C9 of coumarin), 158.13 (C=O of coumarin), 172.21 (S-C=N), 180.55 (C=O); Analysis for C₂₁H₁₈N₄O₅S₂ (470), Calcd.: % C, 53.61; H, 3.86; N, 11.91; O, 17.00; S, 13.63. Found: % C, 53.55; H, 3.83; N, 11.87; O, 16.98; S, 13.60.

2-(4-Oxo-2-(2-(1-(4-(2-oxo-2H-chromene-6-sulfonamido)phenyl)ethylidene)hydrazinyl)-4,5-dihydrothiazol-5-yl)acetic acid (15c)

White crystals, mp 193–194 °C, yield (40%). ¹H NMR (400 MHz, CDCl₃) δ ppm: 2.43 (s, 3H, CH₃), 2.86 (t, 1H, *J* = 6.4 Hz CH thiazolidinone), 3.04 (d, 2H, *J* = 12.8 Hz CH₂), 6.58 (d, 1H, *J* = 7.6 Hz, H3 of coumarin), 7.22 (d, 2H, *J* = 6.4 Hz, Ar), 7.53 (d, 1H, *J* = 7.2 Hz, H8 of coumarin), 7.82 (d, 2H, *J* = 6.4 Hz, Ar), 7.95 (dd, 1H, *J* = 6.8 and 2 Hz, H7 of coumarin), 8.16 (d, 1H, *J* = 8 Hz, H4 of coumarin), 8.27 (s, 1H, H5 of coumarin), 10.99 (s, 1H, NH), 11.14 (s, 1H, NH), 13.21 (s, 1H, COOH); ¹³C NMR (100 MHz, CDCl₃); δ ppm: 16.36 (CH₃), 38.04 (CH₂), 42.56 (CH of thiazolidinone), 118.42, 118.59 (2C), 119.51, 128.29, 129.99 (2C), 130.32 (2C), 132.62, 135.63, 142.37, 143.37 (C4 of coumarin), 152.24 (C=N), 156.56 (C9 of coumarin), 159.51 (C=O of coumarin), 165.86 (S-C=N), 172.48 (C=O of COOH), 196.92 (C=O); Analysis for C₂₂H₁₈N₄O₇S₂ (514), Calcd.: % C, 51.35; H, 3.53; N, 10.89; O, 21.77; S, 12.46. Found: % C, 51.30; H, 3.51; N, 10.86; O, 21.74; S, 12.44.

Biological evaluation

In vitro anti-proliferative activity

HepG2 liver cancer, MCF-7 breast cancer and Caco-2 cancer cell lines were obtained from the National Cancer Institute (Cairo, Egypt). Caco-2 cells were grown in DMEM while HepG2 and MCF-7 were grown in RPMI-1640. Media were supplemented with 10% heat-inactivated FBS, 50 units/mL of penicillin and 50 g/mL of streptomycin and maintained at 37 °C in a humidified atmosphere containing 5% CO₂. The cells were maintained as a “monolayer culture” by serial subculturing. Cytotoxicity was determined using the sulforhodamine B (SRB) method as previously described by Skehan et al.⁵⁰ Exponentially growing cells were collected using 0.25% trypsin-EDTA and seeded in 96-well plates at 1000–2000 cells/well in supplemented DMEM medium. After 24 h, cells were incubated for 72 h with various concentrations of the tested

compounds as well as doxorubicin as the reference compound. Following 72 h of treatment, the cells were fixed with 10% tri-chloroacetic acid for 1 h at 4 °C. Wells were stained for 10 min at room temperature with 0.4% SRB dissolved in 1% acetic acid. The plates were air dried for 24 h, and the dye was solubilized with Tris-HCl for 5 min on a shaker at 1600 rpm. The optical density (OD) of each well was measured spectrophotometrically at 564 nm with an ELISA microplate reader (ChroMate-4300, FL, USA). The IC₅₀ values were calculated according to the equation for Boltzmann sigmoidal concentration-response curve using the non-linear regression models (GraphPad, Prism Version 5). The results reported are means of at least three separate experiments. Significant differences were analyzed by one-way ANOVA wherein the differences were considered to be significant at *p* < .05.

ELISA immunoassay

The levels of the apoptotic markers (Bax, caspase-3) and the anti-apoptotic marker (Bcl-2) were examined using ELISA colorimetric kits per the manufacturer's protocol and referring to reported instructions^{51,52}.

Cell cycle analysis

The HepG2 cells were treated with compound **13a** for 24 h (at IC₅₀ concentration), then cells were washed twice with ice-cold phosphate-buffered saline (PBS). Subsequently, the treated cells were collected by centrifugation, fixed in ice-cold 70% (v/v) ethanol, washed with PBS, re-suspended with 0.1 mg/mL RNase, stained with 40 mg/mL PI, and analyzed by flow cytometry using FACS Calibur (Becton Dickinson, BD). The cell cycle distributions were calculated using CellQuest software (Becton Dickinson)⁵³.

Annexin V-FITC apoptosis assay

Phosphatidylserine externalization was measured using Annexin V-FITC/PI apoptosis detection kit (BD Biosciences, San Jose, CA) according to the manufacturer's instructions, as reported earlier⁵³. HepG2 cells were treated with **13a** at defined concentrations for 24 h.

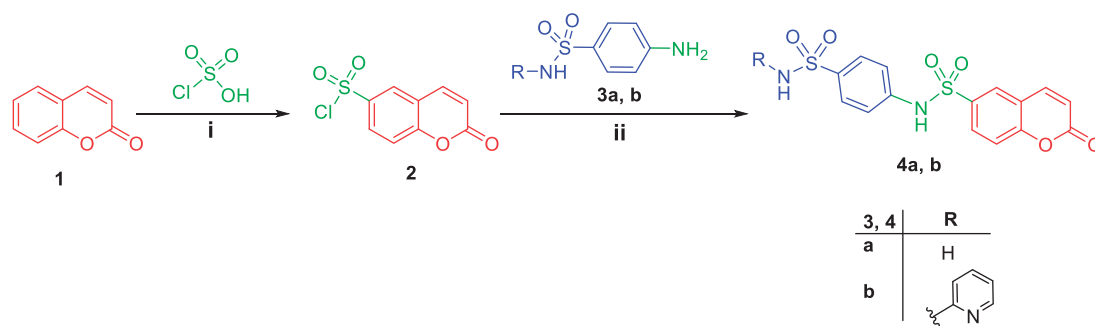
Results and discussion

Chemistry

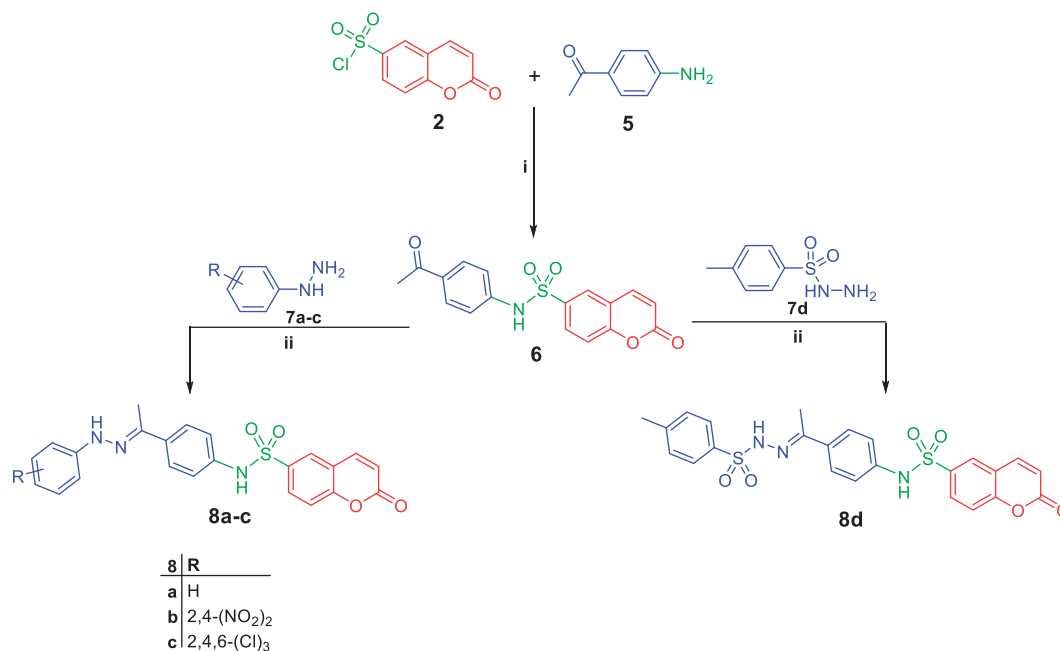
The synthetic routes employed to prepare the new target derivatives are depicted in Schemes 1–4. The key intermediate 2-oxo-2H-chromene-6-sulfonyl chloride **2** was obtained from a reaction of coumarin **1** with chlorosulfonic acid, which subsequently reacted with sulfanilamide **3a** and sulfapyridine **3b** in refluxing ethanol to furnish the corresponding target compounds **4a**, **b**, respectively (Scheme 1).

In Scheme 2, synthesis of *N*-(4-acetylphenyl)-2-oxo-2H-chromene-6-sulfonamide **6** was achieved via stirring compound **2** with 4-aminoacetophenone **5** in dichloromethane at room temperature. The later was refluxed with phenylhydrazine **7a**, 2,4-dinitrophenylhydrazine **7b**, 2,4,6-trichlorophenylhydrazine **7c** and *p*-toluenesulfonyl hydrazide **7d** in absolute ethanol to afford target coumarins **8a–d**.

Refluxing of compound **6** with thiosemicarbazide in ethanol and catalytic amount of acetic acid yielded the key intermediate **9**, which utilized for preparation of diverse derivatives. Treatment of intermediate **9** with the appropriate α -halocarbonyl compounds **10a–d** in refluxing dioxane furnished the corresponding thiazole



Scheme 1. Synthesis of target compounds **4a, b**; *Reagents and conditions*: (i) Heating 100 °C, 4 h; (ii) EtOH/reflux 12 h.



Scheme 2. Synthesis of target compounds **8a–d**; *Reagents and conditions*: (i) Pyridine/stirring, rt 24 h; (ii) EtOH/AcOH (catalytic)/reflux 8 h.

derivatives **11a–d**. Additionally, refluxing of **9** with phenacyl bromide **12a** and coumarin-3-acetyl bromide **12b** in dioxane afforded the corresponding thiazoles **13a, b**, respectively (Scheme 3). Moreover, treatment of intermediate **9** with each of bromoacetic acid **14a**, 2-bromopropanoic acid **14b** and maleic anhydride **14c** in acetic acid in the presence of anhydrous sodium acetate afforded the target thiazolidinone derivatives **15a–c**, respectively (Scheme 4).

Postulated structures of the newly synthesized coumarin sulfonamides were in full agreement with their spectral and elemental analyses data (Supplementary material).

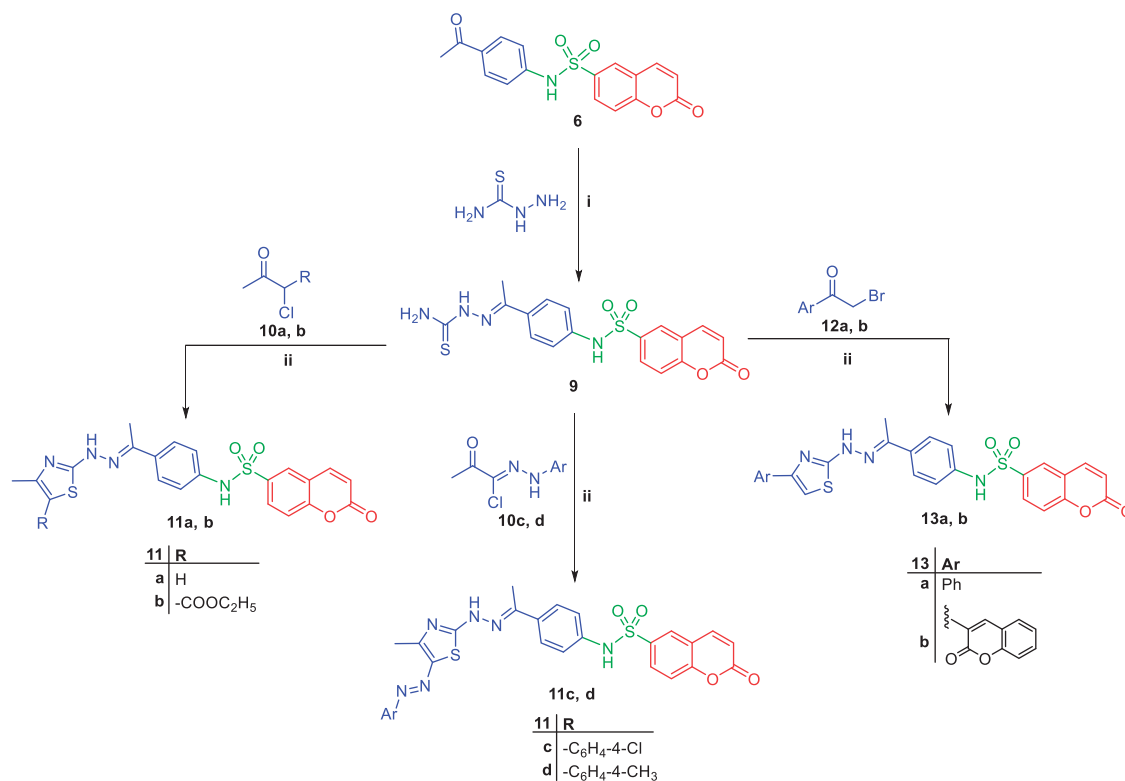
Biological evaluation

In vitro anti-proliferative activity

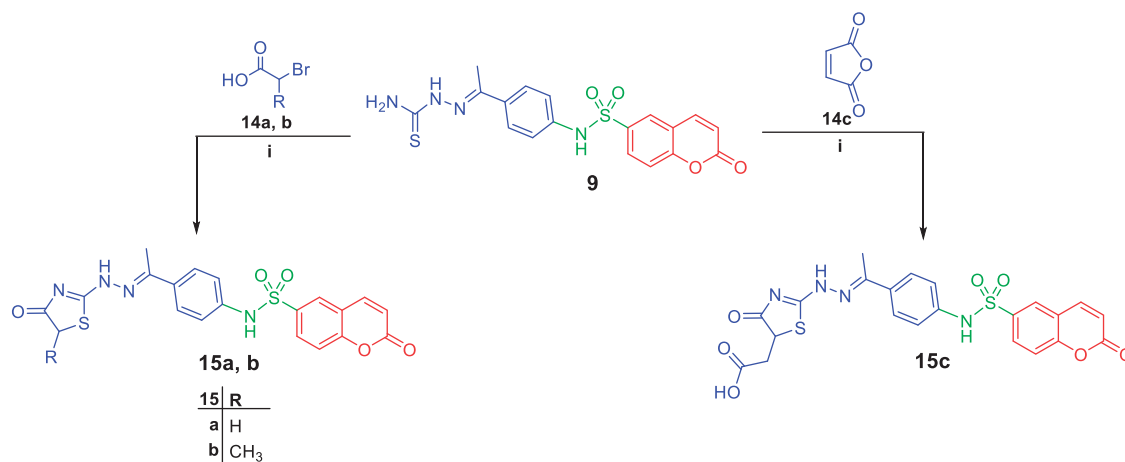
All the newly synthesized target coumarin sulfonamides were evaluated for their *in vitro* anti-proliferative activity against three human tumor cancer cell lines, HepG2 hepatocellular carcinoma, MCF-7 breast cancer, and Caco-2 colon cancer, using SRB colorimetric assay as described by Skehan et al.⁵⁰ Doxorubicin was involved in the experiments as a reference cytotoxic compound. The results were expressed as growth inhibitory concentration (IC₅₀) values which represent the compound concentrations required to produce a 50% inhibition of cell growth after 72 h of incubation compared to untreated controls. The results were summarized in Table 1.

From the displayed results, it was obvious that several of the prepared coumarin sulfonamides possess excellent to modest growth inhibitory activity towards the tested cancer cell lines. Examinations of the anti-proliferative activity towards HepG2 cells revealed that it is the most sensitive cell line to the influence of the target coumarin sulfonamide derivatives. Compounds **13a** and **15a** emerged as the most active coumarins against HepG2 cells through this study with IC₅₀ values of 3.48 ± 0.28 and 5.03 ± 0.39 μ M, respectively. They displayed 1.5- and 1.1-fold increased potency than doxorubicin (IC₅₀ = 5.43 ± 0.24 μ M). Besides, compounds **4b** and **15c** with IC₅₀ values of 8.08 ± 0.51 and 7.57 ± 0.66 μ M, respectively, displayed excellent activity in comparison to doxorubicin. Also, compounds **8b** and **13b** (IC₅₀ = 11.84 ± 1.34 and 11.80 ± 1.16 μ M, respectively) exhibited good anti-proliferative activity. Moreover, compounds **6**, **8a**, **8c**, and **15b** had moderate activity with IC₅₀ values ranging from 25.07 ± 2.08 to 29.80 ± 2.21 μ M.

Concerning activity against MCF-7 cells, compounds **15a** and **15b** were the most active members that displayed potent anti-proliferative activity with IC₅₀ values of 10.95 ± 0.96 and 10.62 ± 1.35 μ M, respectively, in comparison to the standard drug doxorubicin (IC₅₀ = 3.18 ± 0.32 μ M). Moreover, compounds **8a**, **11a**, and **15c** were moderately active against MCF-7 cells with IC₅₀ values: 14.30 ± 1.18 , 13.86 ± 1.19 and 16.32 ± 1.48 μ M, respectively. On the other hand, anti-proliferative activity evaluation in Caco-2 cells showed that compound **8a** possessed the best growth inhibitory



Scheme 3. Synthesis of target compounds **11a–d** and **13a, b**; *Reagents and conditions:* (i) EtOH/ACOH(catalytic)/reflux 6h (ii) Dioxane/TEA (catalytic)/reflux 8h.



Scheme 4. Synthesis of target compounds **15a–c**; *Reagents and conditions:* (i) AcOH/anhydrous AcONa/reflux 8h.

activity ($IC_{50} = 8.53 \pm 0.72$), with twofold decreased activity than doxorubicin ($IC_{50} = 4.10 \pm 1.37 \mu M$). In addition, compound **11a** showed good anti-proliferative activity against Caco-2 cancer cell line ($IC_{50} = 10.12 \pm 0.90$). Whilst, both compounds **8d** and **11d** displayed moderate activity against Caco-2 cancer cell line with IC_{50} values: 16.02 ± 1.32 and 16.06 ± 1.28 , respectively. These results suggest that diverse functionalities could be incorporated into the coumarin sulfonamide scaffold to obtain promising anti-proliferative activity against different types of cancer cells.

In vitro cytotoxicity towards human normal WI-38 cells

The cell growth inhibitory activity of the most potent compounds **13a** and **15a** was examined towards non-tumorigenic human normal lung fibroblast cell line (WI-38) to investigate the potential

safety of the newly synthesized coumarin-6-sulfonamides towards the normal cells. The results were expressed as IC_{50} values, and selectivity index was calculated (Table 2). The tested coumarin-6-sulfonamides (**13a** and **15a**) showed non-significant cytotoxic action with IC_{50} values of 73.20 ± 3.47 and $55.92 \pm 0.39 \mu M$, respectively, with good selectivity index range 21 and 11, thereby providing a high safety profile as anticancer agents.

Apoptosis induction in HepG2 cells

Apoptosis induction in cancer cells represents one of the most successful strategies for the development of cancer therapy^{54–56}. As displayed above, coumarins **13a** and **15a** emerged as the most active ones towards HepG2 liver cancer cells. Accordingly, we investigated the ability of compounds **13a** and **15a** to provoke

Table 1. *In vitro* anti-proliferative activity of the target coumarin sulfonamide derivatives against HepG2, MCF-7 and Caco-2 cancer cell lines.

Compound	IC ₅₀ (μM) ^a		
	HepG2	MCF7	Caco-2
4a	35.48 ± 2.93	50.73 ± 4.61	192.69 ± 15.33
4b	8.08 ± 0.51	22.95 ± 2.04	66.88 ± 6.07
6	25.62 ± 1.36	>200	81.54 ± 6.89
8a	26.99 ± 2.01	14.30 ± 1.18	8.53 ± 0.72
8b	11.84 ± 1.34	126.08 ± 10.87	89.59 ± 7.26
8c	29.80 ± 2.21	>200	76.93 ± 6.59
8d	89.91 ± 7.63	>200	16.02 ± 1.32
9	163.03 ± 10.22	>200	>200
11a	>200	13.86 ± 1.19	10.12 ± 0.90
11b	54.31 ± 3.87	63.42 ± 5.69	145.46 ± 8.02
11c	72.50 ± 6.33	34.73 ± 2.94	108.41 ± 11.36
11d	>200	>200	16.06 ± 1.28
13a	3.48 ± 0.28	83.23 ± 6.85	83.43 ± 7.04
13b	11.80 ± 1.16	>200	96.64 ± 5.37
15a	5.03 ± 0.39	10.95 ± 0.96	158.38 ± 9.39
15b	25.07 ± 2.08	10.62 ± 1.35	174.91 ± 12.30
15c	7.57 ± 0.66	16.32 ± 1.48	46.06 ± 3.17
Doxorubicin	5.43 ± 0.24	3.18 ± 0.32	4.10 ± 1.37

^aIC₅₀ values are the mean ± SE of three separate experiments.

Table 2. *In vitro* cytotoxic activity against normal WI-38 cells, and selectivity index of the most active coumarins.

Compound	IC ₅₀ (μM)		Selectivity index
	WI-38	HepG2	
13a	73.20 ± 3.47	3.48 ± 0.28	21
15a	55.92 ± 0.39	5.03 ± 0.39	11

apoptosis in HepG2 cells to define the principle mechanism for their anti-proliferative activity.

Effects on mitochondrial apoptosis pathway proteins Bcl-2 and Bax

The Bcl-2 proteins family is mainly responsible for synchronizing the mitochondrial apoptotic pathway, and classified into two major classes: anti-apoptotic proteins such as Bcl-2 protein and the counteracting pro-apoptotic proteins including Bax protein. In this study, we examined the impact of coumarins **13a** and **15a** on the level of the anti-apoptotic Bcl2 and the level of the pro-apoptotic Bax (Table 3). As shown in Table 3, compound **13a** induced the protein expression of Bax with 16.5 folds of the control while 14.3 folds were recorded for compound **15a**. On the other hand, treatment of HepG2 cells with compounds **13a** and **15a** significantly reduced the expression levels of the anti-apoptotic protein Bcl-2 by 21.4 and 38.6%, respectively, compared to the control.

Effects on the levels of active caspase-3 (key executor of apoptosis)

As a key executioner protease, caspase-3 is activated by upstream initiator caspases as caspase-9. Herein, treatment of HepG2 cells with coumarins **13a** and **15a** resulted in a significant elevation in the level of active caspase-3 by about 6.6 and 5.7 folds, respectively, compared to control (Table 3).

Cell-cycle analysis

The impact of compound **13a** on cell cycle progression was examined in HepG2 cancer cell line after 24 h of treatment (Figure 2). This impact was illustrated by DNA flow cytometric analysis where

Table 3. Effect of compounds **13a** and **15a** on the active caspase-3 level, and the expression levels of Bcl-2 and Bax in HepG2 cancer cells treated with each compound at its IC₅₀ concentration.

Compound	Caspase-3 (ng/mg protein)	Bax (Pg/mg protein)	Bcl-2 (ng/mg protein)
	(fold)	(fold)	(fold)
13a	0.3021 (6.6) ^a	453.3 (16.5) ^a	1.51 (0.21) ^a
15a	0.2625 (5.7) ^a	394.3 (14.3) ^a	2.73 (0.39) ^a
Control	0.0457	27.52	7.07

^aNumbers given between parentheses are the numbers of folds of control.

HepG2 cells were treated with **13a** at concentration equals to its IC₅₀. Figure 2 showed that exposure of HepG2 cells to compound **13a** induced a significant increase in the percentage of cells at Pre-G1 by 6.4-folds, with concurrent significant arrest in the G2-M phase by 5.4-folds compared to control. Alteration of the Pre-G1 phase and arrest of G2-M phase were significant remarks for compound **13a** to induce apoptosis in HepG2 cells.

Annexin V-FITC apoptosis assay

The apoptotic effect of coumarin **13a** was further assured by Annexin V-FITC/PI (AV/PI) dual staining assay to investigate the occurrence of phosphatidylserine externalization (Figure 3). Flow cytometric analysis revealed that HepG2 cells treated with **13a** showed a significant increase in the percent of annexin V-FITC positive apoptotic cells (UR + LR) from 1.75% to 13.76% which comprises about 7.9 folds compared to control.

2D QSAR study

Development of QSAR models. With the aim to assess the structural basis for the anti-proliferative activity of the newly prepared coumarin sulfonamides (**4a**, **b**, **6**, **8a-d**, **9**, **11a-d**, **13a**, **b** and **15a-c**), 2D-QSAR analysis was carried out. This analysis was run by means of the DS 4.0 software (Discovery Studio 4.0, Accelrys, Co. Ltd)⁵⁷. A set of the newly synthesized compounds (**4a**, **b**, **6**, **8a-d**, **9**, **11a-d**, **13a**, **b** and **15a-c**) was used as training set with their measured pIC₅₀ against **HepG2** and **Caco-2** for QSAR modeling, compounds **6**, **8d**, **15a** and **15c** were chosen as statistical outliers while building model for **HepG2** whereas, compounds **6**, **9**, and **13a** were chosen for the **Caco-2** model.

"Calculate Molecular Properties" module was used for calculating the molecular properties. Genetic function approximation (GFA) protocol was applied in order to choose the best descriptors that characterize the activity. Multiple linear regression (MLR) protocol was then employed to search for optimal QSAR models with the best statistical validation measures and capable of correlating bioactivity variation across the used training set collection. QSAR model was validated employing leave one-out cross-validation by setting the folds to a number much larger than the number of samples, *r*² (squared correlation coefficient value) and *r*² prediction (predictive squared correlation coefficient value), residuals between the predicted and experimental activity of the test set and training set (Table 4).

QSAR study results

Equation (1) Represents the best performing QSAR model for the activity against **HepG2**;

$$-\log \text{IC}_{50} = -0.7926 - 1.598 \text{CHI}_3\text{C} + 0.2775 \text{Dipole}_y - 3.102e - 002 \text{JursPNSA}_3 + 0.04829 \text{Shadow}_{yz} \quad (1)$$

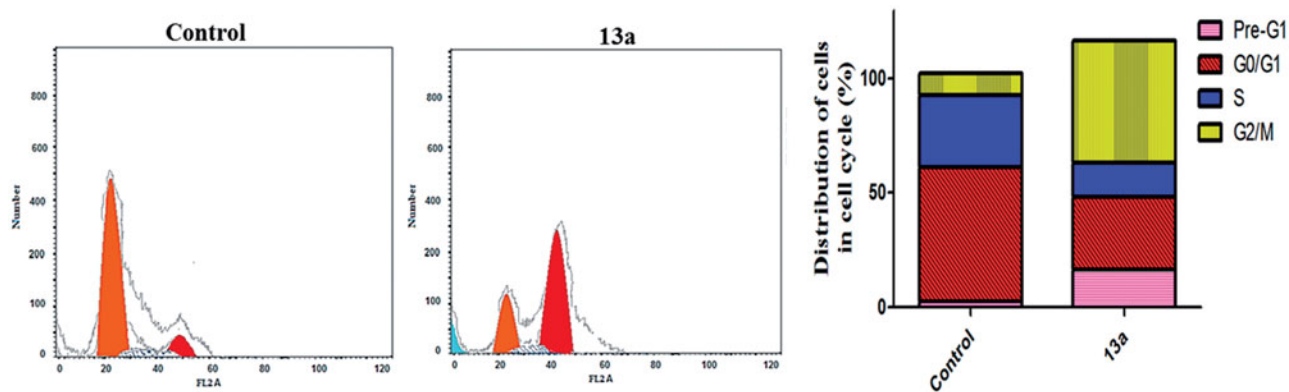


Figure 2. Effect of compound 13a on the phases of cell cycle of HepG2 cells.

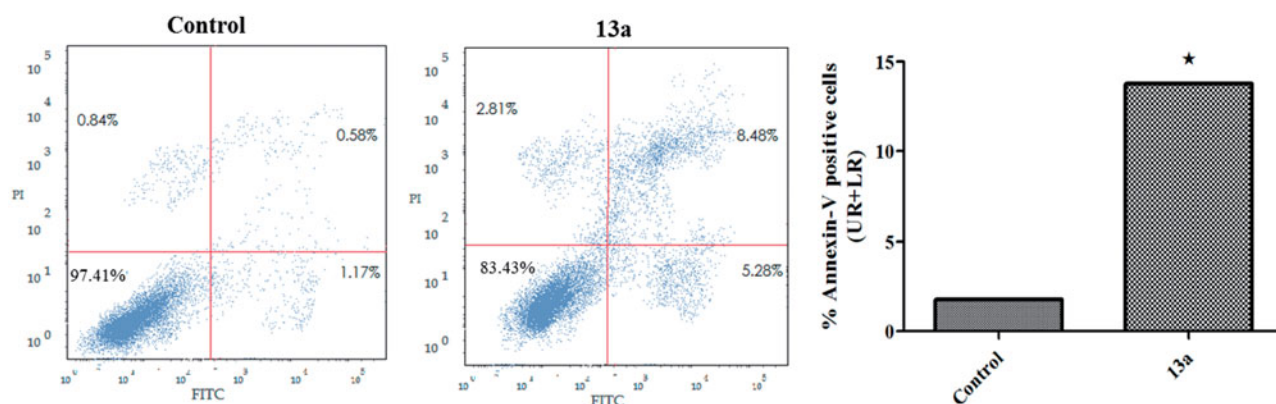


Figure 3. Effect of compound 13a on the percentage of annexin V-FITC-positive staining in HepG2 cells. The experiments were done in triplicates. The four quadrants identified as: LL, viable; LR, early apoptotic; UR, late apoptotic; UL, necrotic. *Significantly different from control at $p < .05$.

Table 4. Experimental activities of the synthesized derivatives against the predicted activity according to Equations (1) and (2).

Compound	Caco-2			HepG2		
	Experimental activity (pIC_{50})	Predicted activity (pIC_{50})	Residual	Experimental activity (pIC_{50})	Predicted activity (pIC_{50})	Residual
4a	-2.2849	-2.2003	-0.0845	-1.5500	-1.5052	-0.0447
4b	-1.8253	-2.0638	0.2385	-0.9074	-0.9211	0.0137
6	—	—	—	—	—	—
8a	-0.9309	-0.8882	-0.0427	-1.4312	-1.5247	0.0935
8b	-1.9523	-1.9601	0.0078	-1.0734	-1.0444	-0.0290
8c	-1.8861	-1.8261	-0.0600	-1.4742	-1.6672	0.1930
8d	-1.2047	-1.1348	-0.0699	—	—	—
9	—	—	—	-2.2123	-2.1558	-0.0565
11a	—	—	—	-2.3118	-2.1523	-0.1595
11b	-2.1627	-2.1391	-0.0237	-1.7349	-1.9201	0.1852
11c	-2.0351	-2.0812	0.0462	-1.8603	-1.9921	0.1317
11d	-1.2058	-1.5517	0.3459	-2.3222	-2.2134	-0.1088
13a	-1.9213	-1.8689	-0.0524	-0.5416	-0.6399	0.0983
13b	-1.9852	-1.7932	-0.1920	-1.0719	-1.0082	-0.0637
15a	-2.1997	-2.1829	-0.0168	—	—	—
15b	-2.2428	-2.1671	-0.0757	-1.3992	-1.1459	-0.2533
15c	-1.6633	-1.6425	-0.0208	—	—	—

Equation (2) Represents the best performing QSAR model for the activity against **Caco-2**;

$$-\log IC_{50} = -6.6095 - 3.7896 IAC_{Mean} + 0.11713 Dipole_X - 0.1615 Shadow_{Ylength} \quad (2)$$

According to the former equations these QSAR models were represented graphically by scattering plots of the experimental

versus the predicted bioactivity values $-\log IC_{50}$ for the training set compounds as shown in Figures 4 and 5.

The two MLR models exhibited good correlation coefficient r^2 of 0.940 and 0.896, r^2 (adj) = 0.910 and 0.865, respectively, r^2 (pred) = 0.878 and 0.789, Least-Squared error = 0.0168 and 0.0173 respectively, where r^2 (adj) is r^2 adjusted for the number of terms in the model; r^2 (pred) is the prediction r^2 , equivalent to q^2 from a leave-1-out cross-validation⁵⁸.

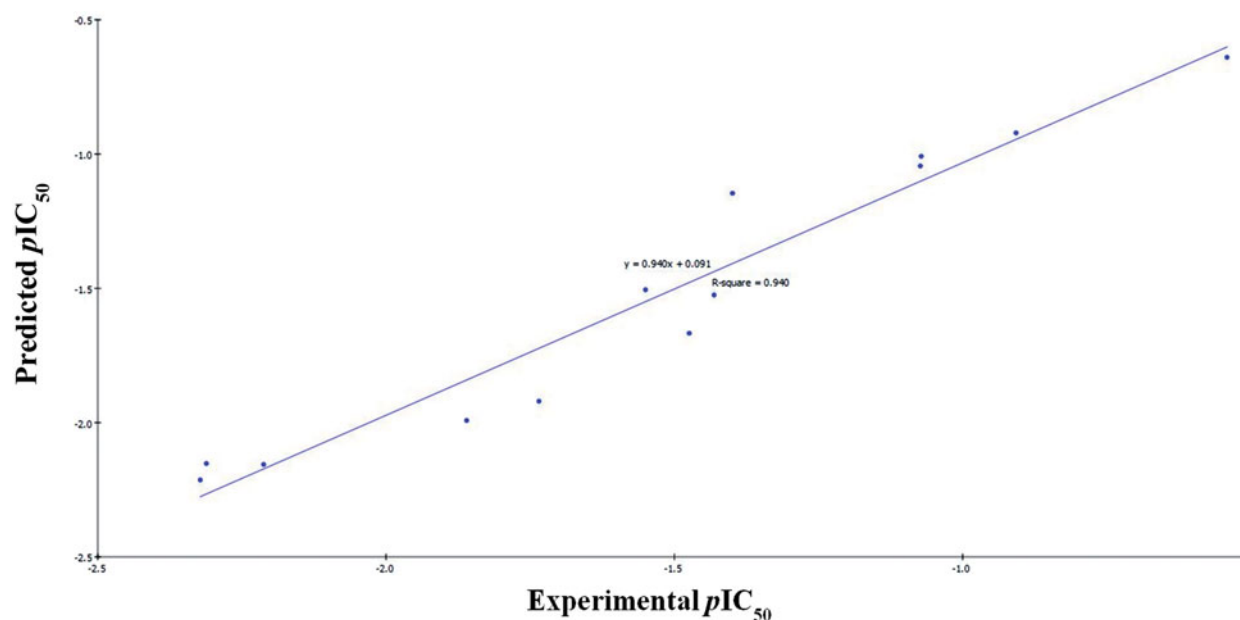


Figure 4. Predicted versus experimental pIC_{50} of the tested compounds against HepG2 according to Equation (1) ($r^2 = 0.940$).

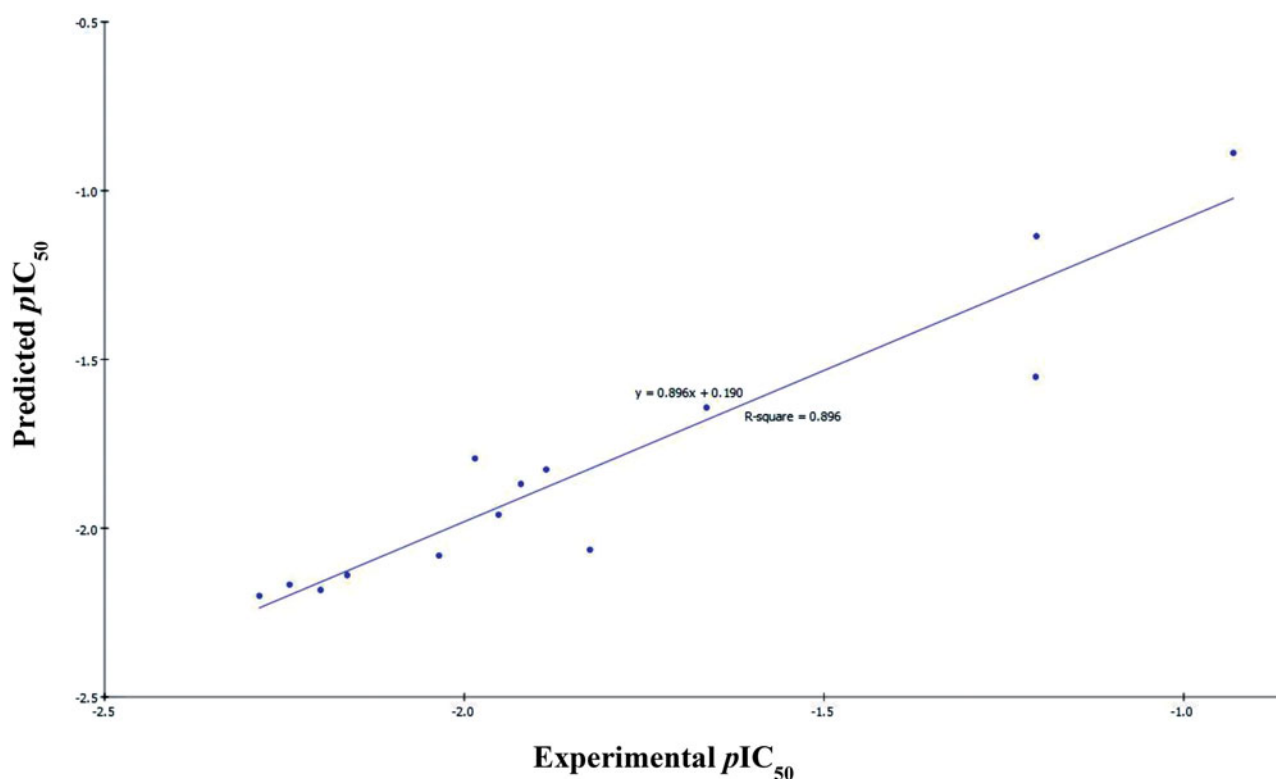


Figure 5. Predicted versus experimental pIC_{50} of the tested compounds against Caco-2 according to Equation (2) ($r^2 = 0.896$).

Equations (1) and (2) for **HepG2** and **Caco-2** suggested that the anti-proliferative activity of the prepared compounds was positively affected by Dipole, which is a 3D electronic descriptors describing the strength and orientation behavior of a molecule in an electrostatic field. Both the magnitude and the components (X, Y, Z) of the dipole moment are calculated (Debyes). It is estimated by utilizing partial atomic charges and atomic coordinates. Partial atomic charges are computed using Gasteiger if not present. Dipole properties have been correlated to long range ligand-receptor recognition and subsequent binding. The

anti-proliferative activity towards **HepG2** was also affected by the high and negative value of Shadow_YZfrac while for **Caco-2** affected by Shadow_Ylength. Shadow indices are a set of geometric descriptors that characterize the shape of the molecules. They are calculated by projecting the model surface on three mutually perpendicular planes: xy, yz, and xz. These descriptors depend not only on conformation, but also on the orientation of the model. In order to calculate them, the models are first rotated to align the principal moments of inertia with the x-, y-, and z-axes. Shadow_YZ is area of the molecular shadow in the yz plane while

Table 5. External validation for the established QSAR models.

Compound	Caco-2			HepG2		
	Experimental activity (pIC ₅₀)	Predicted activity (pIC ₅₀)	Residual	Experimental activity (pIC ₅₀)	Predicted activity (pIC ₅₀)	Residual
6	−1.9114	−1.8158	−0.0956	−1.4086	−0.9815	−0.4271
8d	—	—	—	−1.9538	−1.9191	−0.0347
9	−2.3424	−1.7150	−0.6275	—	—	—
13a	−1.0052	−1.7283	0.7231	—	—	—
15a	—	—	—	−0.7016	−0.8816	0.1801
15c	—	—	—	−0.8791	−1.1608	0.2817

Shadow_Ylength is indicator for length of molecule in the y dimension⁵⁹.

Equation (1) also showed that the anti-proliferative activity was also affected by jurs descriptors. Jurs descriptors are a group of geometric descriptors that combine both shape and electronic information which may characterize the molecules⁶⁰. In particular, Jurs_PNSA_3, which contributes inversely to the activity, represents the atomic charge weighted negative surface area and calculated by Sum of the product of solvent-accessible surface area × partial charge for all negatively charged atoms. This indicates increasing this value in a molecule could increase reuptake inhibition activity because it is negatively correlated with the activity. Equations (1) and (2) are also affected by topological descriptors which are a special class of descriptors that do not rely on a three-dimensional model. All calculations are derived from the two-dimensional topology of the molecule. As CHI_3_C which is connectivity indices while IAC_Mean indicate Graph-Theoretical InfoContent descriptors.

QSAR validation

The established QSAR models (1 and 2) were verified by applying; Leave-one-out (LOO) internal validation ($r^2 = 0.940$ and 0.896 , respectively). Cross-validation was also employed where q^2 , which is equivalent to r^2 (pred), was 0.878 and 0.789 , respectively. In addition, validation was employed by measuring the residuals between the experimental and the predicted activities of the training set listed in Table 4. Interestingly, the predicted activities of the QSAR models were found very close to those experimentally observed. Furthermore, to evaluate the predictive ability of the developed models HepG2, compounds **6**, **8d**, **15a**, and **15c** were applied as test compounds, where they were not included in model generation, the same was also applied for the Caco-2 model using compounds **6**, **9**, and **13a** (Table 5).

Conclusion

In our endeavor to develop potent anti-cancer agents, different sets of coumarin-6-sulfonamide derivatives (**4a**, **b**, **8a–d**, **11a–d**, **13a**, **b**, and **15a–c**) were synthesized. Anti-proliferative activities of the newly synthesized coumarins was investigated in three human tumor cancer cell lines, namely, HepG2 hepatocellular carcinoma, MCF-7 breast cancer and Caco-2 colon cancer using sulforhodamine B (SRB) colorimetric assay. Compounds **13a** and **15a** emerged as the most active derivatives towards HepG2 cells ($IC_{50} = 3.48 \pm 0.28$ and $5.03 \pm 0.39 \mu M$, respectively), with 1.5- and 1.1-fold increased activity than the reference drug, doxorubicin ($IC_{50} = 6.9 \pm 2.05 \mu M$), respectively. Besides, compounds **15a** and **15b** were the most active members against MCF-7 cells with IC_{50} values of 10.95 ± 0.96 and $10.62 \pm 1.35 \mu M$, respectively. Also, compound **8a** possessed the best growth inhibitory activity against Caco-2 cells ($IC_{50} = 8.53 \pm 0.72$), with 2-fold decreased activity than

doxorubicin ($IC_{50} = 4.10 \pm 1.37 \mu M$). Compounds **13a** and **15a** were able to induce apoptosis in HepG2 cells, as assured by the up-regulation of the Bax and down-regulation of the Bcl-2, besides boosting caspase-3 levels. Besides, compound **13a** induced a significant increase in the percentage of cells at Pre-G1 by 6.4-folds, with concurrent significant arrest in the G2-M phase by 5.4-folds compared to control. Also, **13a** displayed significant increase in the percentage of annexin V-FITC positive apoptotic cells from 1.75% to 13.76%. Moreover, QSAR models were established to explore the structural requirements controlling the anti-proliferative activities.

Disclosure statement

No potential conflict of interest was reported by the authors.

References

1. Miller KD, Siegel RL, Lin CC, et al. Cancer treatment and survivorship statistics. *CA Cancer J Clin* 2016;66:271–89.
2. Grover J, Jachak SM. Coumarins as privileged scaffold for anti-inflammatory drug development. *RSC Adv* 2015;5:38892–905.
3. Al-Majedy Y, Kadhum AA, Ibraheem H, et al. A systematic review on pharmacological activities of 4-methylumbelliferon. *Sys Rev Pharm* 2018;8:24–30.
4. Hassan MZ, Osman H, Ali MA, Ahsan MJ. Therapeutic potential of coumarins as antiviral agents. *Eur J Med Chem* 2016;123:236–55.
5. Pinto DC, Silva AM. Anticancer natural coumarins as lead compounds for the discovery of new drugs. *Curr Top Med Chem* 2017;17:3190–98.
6. Thakur A, Singla R, Jaitak V. Coumarins as anticancer agents: a review on synthetic strategies, mechanism of action and SAR studies. *Eur J Med Chem* 2015;101:476–95.
7. Kaur M, Kohli S, Sandhu S, et al. Coumarin: a promising scaffold for anticancer agents. *Anticancer Agents Med Chem* 2015;15:1032–48.
8. Dandriyal J, Singla R, Kumar M, Jaitak V. Recent developments of C-4 substituted coumarin derivatives as anticancer agents. *Eur J Med Chem* 2016;119:141–68.
9. Degorce SL, Bailey A, Callis R, et al. Investigation of (E)-3-[4-(2-Oxo-3-aryl-chromen-4-yl) oxyphenyl] acrylic acids as oral selective estrogen receptor down-regulators. *J Med Chem*. 2015;58:3522–33.
10. Civelli M, Preti AP, Cenacchi V, et al. Single and multiple ascending dose studies of a novel tissue-selective oestrogen receptor modulator, CHF 4227, in healthy postmenopausal women. *Br J Clin Pharmacol*. 2007;64:304–16.
11. Suzuki N, Liu X, Laxmi YR, et al. Anti-breast cancer potential of SS5020, a novel benzopyran antiestrogen. *Int J Cancer*. 2011;128:974–82.

12. Liu MM, Chen XY, Huang YQ, et al. Hybrids of phenylsulfonylfuroxan and coumarin as potent antitumor agents. *J Med Chem*. 2014;57:9343–56.
13. Wang C, Xu F, Niu Y, et al. Synthesis and biological evaluations of 3-benzothiazol-2-yl coumarin derivatives as MEK1 inhibitors. *Lett Drug Des Discov*. 2013;10:727–32.
14. Han S, Zhou V, Pan S, et al. Identification of coumarin derivatives as a novel class of allosteric MEK1 inhibitors. *Bioorg Med Chem Lett*. 2005;15:5467–73.
15. Palmieri C, Januszewski A, Stanway S, Coombes RC. Irosustat: a first-generation steroid sulfatase inhibitor in breast cancer. *Expert Rev. Anticancer Ther*. 2011;11:179–83.
16. Daško M, Przybyłowska M, Rachon J, et al. Synthesis and biological evaluation of fluorinated N-benzoyl and N-phenylacetoyl derivatives of 3-(4-aminophenyl)-coumarin-7-O-sulfamate as steroid sulfatase inhibitors. *Eur J Med Chem*. 2017;128:79–87.
17. Demkowicz S, Daško M, Kozak W, et al. Synthesis and biological evaluation of fluorinated 3-phenylcoumarin-7-O-sulfamate derivatives as steroid sulfatase inhibitors. *Chem Biol Drug Des*. 2016;87:233–8.
18. Bana E, Sibille E, Valente S, et al. A novel coumarin-quinone derivative SV37 inhibits CDC25 phosphatases, impairs proliferation, and induces cell death. *Mol Carcinog*. 2015;54:229–41.
19. Zwergel C, Czepukojc B, Evain-Bana E, et al. Novel coumarin- and quinolinone-based polycycles as cell division cycle 25-A and-C phosphatases inhibitors induce proliferation arrest and apoptosis in cancer cells. *Eur J Med Chem*. 2017;134:316–33.
20. Valente S, Bana E, Viry E, et al. Synthesis and biological evaluation of novel coumarin-based inhibitors of Cdc25 phosphatases. *Bioorg Med Chem Lett*. 2010;20:5827–30.
21. Cao D, Liu Y, Yan W, et al. Design, synthesis, and evaluation of in vitro and in vivo anticancer activity of 4-substituted coumarins: a novel class of potent tubulin polymerization inhibitors. *J Med Chem*. 2016;59:5721–39.
22. Singh H, Kumar M, Nepali K, et al. Triazole tethered C5-curcuminoid-coumarin based molecular hybrids as novel antitubulin agents: Design, synthesis, biological investigation and docking studies. *Eur J Med Chem*. 2016;116:102–15.
23. Samundeeswari S, Kulkarni MV, Joshi SD, et al. Synthesis and human anticancer cell line studies on coumarin- β -carboline hybrids as possible antimetabolic agents. *ChemistrySelect*. 2016;1:5019–24.
24. Ghorab MM, Alsaid MS, Al-Ansary GH, et al. Analogue based drug design, synthesis, molecular docking and anticancer evaluation of novel chromene sulfonamide hybrids as aromatase inhibitors and apoptosis enhancers. *Eur J Med Chem*. 2016;124:946–58.
25. Chen S, Cho M, Karlsberg K, et al. Biochemical and biological characterization of a novel anti-aromatase coumarin derivative. *J Biol Chem*. 2004;279:48071–8.
26. Lu XY, Wang ZC, Ren SZ, et al. Coumarin sulfonamides derivatives as potent and selective COX-2 inhibitors with efficacy in suppressing cancer proliferation and metastasis. *Bioorg Med Chem Lett*. 2016;26:3491–8.
27. (a) Avin BV, Thirusangu P, Ranganatha VL, et al. Synthesis and tumor inhibitory activity of novel coumarin analogs targeting angiogenesis and apoptosis. *Eur J Med Chem*. 2014;75:211–21. (b) Lin MH, Cheng CH, Chen KC, et al. Induction of ROS-independent JNK-activation-mediated apoptosis by a novel coumarin-derivative, DMAC, in human colon cancer cells. *Chem-Biol Interact*. 2014;218:42–9.
28. (a) Han HW, Zheng CS, Chu SJ, et al. The evaluation of potent antitumor activities of shikonin coumarin-carboxylic acid, PMMB232 through HIF-1 α -mediated apoptosis. *Biomed Pharmacother*. 2018;97:656–66. (b) Lopez-Gonzalez JS, Prado-Garcia H, Aguilar-Cazares D, et al. Apoptosis and cell cycle disturbances induced by coumarin and 7-hydroxycoumarin on human lung carcinoma cell lines. *Lung cancer*. 2004;43:275–83.
29. (a) Wang Q, Guo Y, Jiang S, et al. A hybrid of coumarin and phenylsulfonylfuroxan induces caspase-dependent apoptosis and cytoprotective autophagy in lung adenocarcinoma cells. *Phytomedicine*. 2017;160–67. (b) Perumalsamy H, Sankarapandian K, Veerapan K, et al. In silico and In vitro analysis of coumarin derivative induced anticancer effects by undergoing intrinsic pathway mediated apoptosis in human stomach cancer. *Phytomedicine*. 2018.
30. (a) Mirunalini S, Deepalakshmi K, Manimozhi J. Antiproliferative effect of coumarin by modulating oxidant/antioxidant status and inducing apoptosis in Hep2 cells. *Biomed Aging Path*. 2014;4:131–5. (b) Domracheva I, Kanepe-Lapsa I, Jackevica L, et al. Selenopheno quinolinones and coumarins promote cancer cell apoptosis by ROS depletion and caspase-7 activation. *Life Sci*. 2017;186:92–101.
31. (a) Ma YM, Zhou YB, Xie CM, et al. Novel microtubule-targeted agent 6-chloro-4-(methoxyphenyl) coumarin induces G 2-M arrest and apoptosis in HeLa cells. *Acta Pharmacol Sin*. 2012;33:407–17. (b) Álvarez-Delgado C, Reyes-Chilpa R, Estrada-Muñiz E, et al. Coumarin A/AA induces apoptosis-like cell death in HeLa cells mediated by the release of apoptosis-inducing factor. *J Biochem Mol Toxicol*. 2009;23:263–72.
32. (a) Scozzafava A, Mastrolorenzo A, Supuran CT. Sulfonamides and sulfonylated derivatives as anticancer agents. *Curr Cancer Drug Targets* 2002;2:55–75. (b) Uehara T, Minoshima Y, Sagane K, et al. Selective degradation of splicing factor CAPER α by anticancer sulfonamides. *Nat Chem Biol* 2017; 13:675.
33. (a) Eldehna WM, Abo-Ashour MF, Nocentini A, et al. Novel 4/3-((4-oxo-5-(2-oxoindolin-3-ylidene) thiazolidin-2-ylidene) amino) benzenesulfonamides: Synthesis, carbonic anhydrase inhibitory activity, anticancer activity and molecular modelling studies. *Eur J Med Chem* 2017;139:250–62. (b) Fares M, Eladwy RA, Nocentini A, et al. Synthesis of bulky-tailed sulfonamides incorporating pyrido [2, 3-d][1, 2, 4] triazolo [4, 3-a] pyrimidin-1 (5H)-yl moieties and evaluation of their carbonic anhydrases I, II, IV and IX inhibitory effects. *Bioorg Med Chem*. 2017;25:2210–7. (c) Alafeefy AM, Ahmad R, Abdulla M, et al. Development of certain new 2-substituted-quinazolin-4-yl-aminobenzenesulfonamide as potential antitumor agents. *Eur J Med Chem* 2016;109:247–53. (d) Eldehna WM, Fares M, Ceruso M, et al. Amido/ureidosubstituted benzene-sulfonamides-isatin conjugates as low nanomolar/subnanomolar inhibitors of the tumor-associated carbonic anhydrase isoform XII. *Eur J Med Chem* 2016;110:259–66. (e) Eldehna WM, Al-Ansary GH, Bua S, et al. Novel indolin-2-one-based sulfonamides as carbonic anhydrase inhibitors: Synthesis, in vitro biological evaluation against carbonic anhydrases isoforms I, II, IV and VII and molecular docking studies. *Eur J Med Chem* 2017;127:521–30.
34. Reddy NS, Mallireddigari MR, Cosenza S, et al. Synthesis of new coumarin 3-(N-aryl) sulfonamides and their anticancer activity. *Bioorg Med Chem Lett* 2004;14:4093–7.
35. Musa MA, Cooperwood JS, Khan MO. A review of coumarin derivatives in pharmacotherapy of breast cancer. *Curr Med Chem* 2008;15:2664–79.

36. Bonardi A, Falsini M, Catarzi D, et al. Structural investigations on coumarins leading to chromeno [4, 3-c] pyrazol-4-ones and pyrano [4, 3-c] pyrazol-4-ones: New scaffolds for the design of the tumor-associated carbonic anhydrase isoforms IX and XII. *Eur J Med Chem* 2018.
37. Chandak N, Ceruso M, Supuran CT, Sharma PK. Novel sulfonamide bearing coumarin scaffolds as selective inhibitors of tumor associated carbonic anhydrase isoforms IX and XII. *Bioorg Med Chem* 2016;24:2882–6.
38. Pacchiano F, Carta F, McDonald PC, et al. Ureido-substituted benzenesulfonamides potently inhibit carbonic anhydrase IX and show antimetastatic activity in a model of breast cancer metastasis. *J Med Chem* 2011;54:1896–902.
39. Safety Study of SLC-0111 in Subjects with Advanced Solid Tumours. See at: <https://clinicaltrials.gov/ct2/show/NCT02215850>.
40. Lou Y, McDonald PC, Oloumi A, et al. Targeting tumor hypoxia: suppression of breast tumor growth and metastasis by novel carbonic anhydrase IX inhibitors. *Cancer Res* 2011;71:3364–76.
41. Wang W, Ao L, Rayburn ER, et al. KCN1, a novel synthetic sulfonamide anticancer agent: in vitro and in vivo anti-pancreatic cancer activities and preclinical pharmacology. *PLoS One* 2012;7:e44883.
42. Yin S, Kaluz S, Devi NS, et al. Arylsulfonamide KCN1 inhibits in vivo glioma growth and interferes with HIF signaling by disrupting HIF-1 α interaction with cofactors p300/CBP. *Clin Cancer Res* 2012.
43. Fukuoka K, Usuda J, Iwamoto Y, et al. Mechanisms of action of the novel sulfonamide anticancer agent E7070 on cell cycle progression in human non-small cell lung cancer cells. *Invest New Drugs* 2001;19:219–27.
44. Ozawa Y, Sugi NH, Nagasu T, et al. E7070, a novel sulphonamide agent with potent antitumor activity in vitro and in vivo. *Eur J Cancer* 2001;37:2275–82.
45. Ozawa Y, Kusano K, Owa T, et al. Therapeutic potential and molecular mechanism of a novel sulfonamide anticancer drug, indisulam (E7070) in combination with CPT-11 for cancer treatment. *Cancer Chemother Pharmacol.* 2012;69:1353–62.
46. Manasa KL. E7010: investigational anticancer agents targeting the microtubules. *Int J Pharm Sci Res.* 2015;6:3713.
47. Assi R, Kantarjian HM, Kadia TM, et al. Final results of a phase 2, open-label study of indisulam, idarubicin, and cytarabine in patients with relapsed or refractory acute myeloid leukemia and high-risk myelodysplastic syndrome. *Cancer*. 2018. (Accepted manuscript, DOI: [10.1002/cncr.31398](https://doi.org/10.1002/cncr.31398))
48. Miller JN. Coumarin-6-sulphonyl chloride: a novel label in fluorimetry and phosphorimetry Part 1. Synthesis and Luminescence Properties. *Anal Chim Acta* 1989;227:145–53.
49. Bary HM, Aleem AH, Ismail II. Reactions with coumarin IV. *Afinidad* 1995;52:344–6.
50. (a) Skehan P, Storeng R, Scudiero D, et al. New colorimetric cytotoxicity assay for anticancer-drug screening. *JNCI: J Natl Cancer Inst* 1990;82:1107–12. (b) Eldehna WM, Fares M, Ibrahim HS, et al. Synthesis and cytotoxic activity of biphenylurea derivatives containing indolin-2-one moieties. *Molecules*. 2016;21(6):762.
51. Eldehna WM, Almahli H, Al-Ansary GH, et al. Synthesis and in vitro anti-proliferative activity of some novel isatins conjugated with quinazoline/phthalazine hydrazines against triple-negative breast cancer MDA-MB-231 cells as apoptosis-inducing agents. *J Enz Inhib Med Chem* 2017; 32:600–13.
52. Almahli H, Hadchity E, Jaballah MY, et al. Development of novel synthesized phthalazinone-based PARP-1 inhibitors with apoptosis inducing mechanism in lung cancer. *Bioorg Chem* 2018;77:443–56.
53. (a) Eldehna WM, EL-Naggar DH, Hamed AR, et al. One-pot three-component synthesis of novel spirooxindoles with potential cytotoxic activity against triple-negative breast cancer MDA-MB-231 cells. *J Enz Inhib Med Chem* 2018;33:309–18. (b) Abdel-Aziz HA, Ghabbour HA, Eldehna WM, et al. 2-((Benzimidazol-2-yl) thio)-1-arylethan-1-ones: Synthesis, crystal study and cancer stem cells CD133 targeting potential. *Eur J Med Chem* 2015;104:1–10.
54. Hu W, Kavanagh JJ. Anticancer therapy targeting the apoptotic pathway. *Lancet Oncol* 2003;4:721–9.
55. Attia MI, Eldehna WM, Afifi SA, et al. New hydrazoneindolin-2-ones: synthesis, exploration of the possible anti-proliferative mechanism of action and encapsulation into PLGA microspheres. *PLoS One* 2017;12:e0181241.
56. (a) Eldehna WM, Ibrahim HS, Abdel-Aziz HA, et al. Design, synthesis and in vitro antitumor activity of novel N-substituted- 4-phenyl/benzylphthalazin-1-ones. *Eur J Med Chem* 2015;89:549–60. (b) Abdel-Aziz HA, Eldehna WM, Ghabbour H, et al. Synthesis, crystal study, and anti-proliferative activity of some 2-benzimidazolylthioacetophenones towards triple-negative breast cancer MDA-MB-468 cells as apoptosis-inducing agents. *Int J Mol Sci.* 2016;17:1221.
57. Discovery Studio 4.0 (Accelrys, Co. Ltd). 2017. <http://www.accelrys.com/> [last accessed 24 July 2017].
58. Mitra I, Saha A, Roy K. Chemometric QSAR modeling and in silico design of antioxidant NO donor phenols. *Sci Pharma* 2010;79:31–58.
59. Behmaram B, Foroughifar N, Foroughifar N, Hallajian S. Synthesis of some derivatives of 4-phenyl-1, 3-dihydro-2H-imidazole-2-thion using ionic liquid as catalyst and evaluation of their antimicrobial activity. *Int J Chem* 2017;9:45.
60. Ghose AK, Crippen GM. Atomic physicochemical parameters for three-dimensional structure-directed quantitative structure-activity relationships I. Partition coefficients as a measure of hydrophobicity. *J Comput Chem* 1986;7:565–77.